



This work is licensed under a Creative Commons Attribution-NonCommercial 4.0 International License. Fonte: <https://www.scielo.br/j/jbsmse/a/w4tZfCGb9NTCGfM4smzQb6y/?lang=en#>. Acesso em: 28 set. 2022.

Referência

GONTIJO, Rafael Gabler; RODRIGUES, José Luiz Alves da Fontoura. The numerical modeling of thermal turbulent wall flows with the classical $\kappa - \epsilon$ model. **Journal of the Brazilian Society of Mechanical Sciences and Engineering**, Rio de Janeiro, v. 33, n. 1, p. 107-116, 2011. DOI: <https://doi.org/10.1590/S1678-58782011000100015>. Disponível em: <https://www.scielo.br/j/jbsmse/a/w4tZfCGb9NTCGfM4smzQb6y/?lang=en#>. Acesso em: 28 set. 2022.

Rafael Gabler Gontijo

rafaelgabler@gmail.com

Universidade de Brasília - Departamento
de Engenharia Mecânica
Vortex - Mecânica dos Fluidos de
Escoamentos Complexos
Brasília
70910-900 DF, Brazil

**José Luiz Alves da Fontoura
Rodrigues**

fontoura@unb.br

Universidade de Brasília - Departamento
de Engenharia Mecânica
Vortex - Mecânica dos Fluidos de
Escoamentos Complexos
Brasília
70910-900 DF, Brazil

The Numerical Modeling of Thermal Turbulent Wall Flows with the Classical $\kappa - \varepsilon$ Model

The goal of this work is to propose a new methodology to simulate turbulent thermal wall flows using the classical $\kappa - \varepsilon$ model. The focus of this approach is based on the manner used to implement heat flux boundary conditions on the solid walls. In order to explain and to validate this new algorithm, several test cases are presented, testing a great range of flows in order to analyze the numerical response on different physical aspects of the fluid flow. The proposed approach uses simultaneously a thermal wall law, an analogy between fluid friction and heat transfer and an interpolating polynomial relation that is constructed with a data base generated on experimental research and numerical simulation. The algorithm used to execute the numerical simulations applies the classical $\kappa - \varepsilon$ model with a consolidated Reynolds and Favre averaging process for the turbulent variables. The turbulent inner layer can be modeled by four distinct velocity wall laws and by one temperature wall law. Spatial discretization is done by P1 and P1/isoP2 finite elements and the temporal discretization is implemented using a semi-implicit sequential scheme of finite differences. The pressure-velocity coupling is numerically solved by a variation of Uzawa's algorithm. To filter the numerical noises, originated by the symmetric treatment of the convective fluxes, it is adopted a balance dissipation method. The remaining nonlinearities, due to explicit calculations of boundary conditions by wall laws, are treated by a minimal residual method.

Keywords: turbulence, finite element method, wall laws, analogies, turbulent heat flux

Introduction

Thermal turbulent flows over solid surfaces occur in many situations of industrial interest and the thermal boundary conditions imposed on the boundaries of the computational grid may be of two types: temperature and/or heat flux. The second condition is more usual in real problems and it brings some additional difficulties to its numerical treatment.

According to Chen and Jaw (1998), the high Reynolds $\kappa - \varepsilon$ model is the most used turbulence model in the treatment of industrial flows. To model the behavior of the flow in the internal region of the turbulent boundary layer, the $\kappa - \varepsilon$ model uses analytical expressions known as wall laws. The main difficulty in simulating a thermal turbulent flow with a heat flux boundary condition on the wall using the high Reynolds $\kappa - \varepsilon$ model is the absence of a heat flux wall law.

The method that we propose to solve this inconvenience is to calculate the convective heat transfer coefficient h , along the solid boundary, and use its value to convert an imposed heat flux on an equivalent wall temperature. This information is then sent to a temperature wall law that calculates the temperature boundary condition in the nodes placed on the border of the computational grid.

The main difficulty is to estimate, with a good accuracy, the numerical values of the convective heat transfer coefficient, since it strongly depends on the flow and on features like the thermodynamical properties of the fluid, the solid geometry in which the flow occurs and the Reynolds number of the flow. In this work, for non-

detached boundary layers, the values of h are calculated with the use of analogies between fluid friction and heat diffusion. For detached boundary layers the calculation is done using an interpolating polynomial relation.

The good performance of classical analogies used to calculate heat transfer rates on flat plates was shown by Gontijo and Fontoura Rodrigues (2006). The problem of using analogies between fluid friction and heat diffusion in detached boundary layers was discussed in the work of Gontijo and Fontoura Rodrigues (2007). An original approach based on the use of analogies for solving the problem of imposing heat flux boundary conditions on the high Reynolds $\kappa - \varepsilon$ model was first presented by Gontijo and Fontoura Rodrigues (2008) and an evolution of this method was shown by Gontijo and Fontoura Rodrigues (2009). The present work shows how this new and original method can be used to simulate thermal turbulent flows with heat flux boundary conditions over different geometries.

The solver used to execute the simulations, named Turbo 2D, is a research Fortran numerical code that has been continuously developed by members of the Group of Complex Fluid Dynamics - Vortex, of the Mechanical Engineering Department of the University of Brasília, in the last twenty years. This solver is based on the adoption of the finite elements technique, under the formulation of weighted residuals proposed by Galerkin, adopting in the spatial discretization of the calculation domain triangular elements of the type P1 and P1-isoP2, as proposed by Brison, Buffat, Jeandel and Serres (1985). The P1-isoP2 mesh is obtained dividing each element of the P1 mesh into four new elements. In the P1 mesh only the pressure field is calculated, while all the other turbulent variables are calculated with the P1-isoP2 mesh.

Paper accepted August, 2010. Technical Editor: Eduardo Morgado Belo

Considering the uncertainties normally existing about the initial condition of the flow field, it is adopted a temporal integration scheme of the governing equations system. In the temporal integration process, the initial state corresponds to the beginning of the flow and the final state occurs when temporal variations of velocity, pressure, temperature and other turbulent variables stop. In order to reach the final state a pseudo transient occurs. The temporal discretization of the governing equations is implemented by the algorithm of Brun (1988), which uses a sequential semi-implicit finite differences method with truncation error of order $O(\Delta t)$ and allows a linear handling of the equation system, at each time step.

The resolution of the coupled equations of continuity and momentum is done by a variant of Uzawa's algorithm, proposed by Buffat (1981). The statistical formulation, used for obtaining the system of average equations, is done with the simultaneous employment of the Reynolds (1895) and Favre (1965) decomposition. The Reynolds stress tensor is calculated by the hypothesis of the turbulent viscosity of Boussinesq (1877), which is modeled by the $\kappa - \varepsilon$ model, proposed by Jones and Launder (1972) with the modifications introduced by Launder and Spalding (1974). The turbulent heat flux is modeled algebraically using a turbulent Prandtl number with a constant value of 0.9.

In the program Turbo 2D, the boundary conditions of velocity and temperature can be calculated by four velocity and two temperature wall laws. The velocity wall functions used in this work are: the classical logarithm law, and the laws of Mellor (1966), Nakayama and Koyama (1984), and Cruz and Silva Freire (1998). The temperature wall law used is the Cheng and Ng (1982) law. The numerical instability resultant of the explicit calculation of velocity boundary conditions is controlled by the algorithm proposed by Fontoura Rodrigues (1990). The numerical oscillations induced by the Galerkin formulation, resultant of the centered discretization applied to a parabolic phenomenon, are cushioned by the technique of balanced dissipation, proposed by Huges and Brooks (1979) and Kelly, Nakazawa and Zienkiewicz (1976) with the numerical algorithm proposed by Brun (1988).

In order to validate and quantify the consistence of the present research code, the numerical results are compared with an extensive experimental database, including several flows over distinct geometries, based on the works of Ng (1981), Vogel and Eaton (1985), Taylor et al. (1990), Liou et al. (1992), Buice and Eaton (1995) and Loureiro et al. (2007).

Nomenclature

t	time variable
x_i	spacial variable - component in the i direction
u_i	fluid velocity
\tilde{u}_i	velocity's mean value by Favre's decomposition
u_i''	velocity fluctuation by Favre's decomposition
u_∞	velocity of the free stream flow
u_f	friction velocity
T	fluid temperature
\tilde{T}	temperature's mean value by Favre's decomposition
T_∞	temperature of the free stream flow

T_f	friction temperature
T_w	wall temperature
p	pressure
\bar{p}	mean pressure by Favre's decomposition
q_i''	heat flux vector
q_w''	heat flux on the wall
k	fluid's thermal conductivity
C_p	specific heat at constant pressure
g_i	gravitational acceleration vector
$\frac{D}{Dt}$	Material's derivative operator
R	ideal gas constant
K	Von Karman's constant
α	fluid's thermal conductivity
α_t	turbulent thermal conductivity
ρ	fluid's density
$\bar{\rho}$	density mean value by Reynolds decomposition
ρ''	density's fluctuations
τ_{ij}	shear stress tensor in indicial notation
τ_w	shear stresses on the wall
κ	turbulent kinetic energy
ε	dissipation of turbulent kinetic energy
ν	kinematic viscosity
ν_t	dynamic turbulent viscosity
μ	dynamic viscosity
μ_t	turbulent dynamic viscosity
β	volumetric expansion coefficient
δ_{ij}	Kronecker's delta operator
Fr	Froude number
Ma	Mach number
Nu	Nusselt number
Pr	Prandtl number
Pr_t	turbulent Prandtl number
Re	Reynolds number
Re_t	turbulent Reynolds number
St	Stanton number
y^+	Reynolds number of the turbulent boundary layer

Theoretical Formulation

Governing Equations

In this work all the dependent variables of the fluid are treated as a time average value plus a fluctuation in a determinate point of space and time. In order to account variations of density, the model applies the well known Reynolds (1985) decomposition to pressure and fluid density and the Favre (1965) decomposition to velocity and temperature. In the Favre (1965) decomposition a generic variable φ is defined as:

$$\varphi(\vec{x}, t) = \tilde{\varphi}(\vec{x}) + \varphi''(\vec{x}, t)$$

with

$$\tilde{\varphi} = \frac{\overline{\rho\varphi}}{\bar{\rho}} \quad \text{and} \quad \overline{\varphi''(\vec{x}, t)} \neq 0. \quad (1)$$

Applying the Reynolds (1895) and Favre (1965) decompositions to the governing equations and taking the time average value of those equations, we obtain the mean Reynolds equations:

$$\frac{\partial \bar{\rho}}{\partial t} + \frac{\partial}{\partial x_i} (\bar{\rho} \tilde{u}_i) = 0, \quad (2)$$

$$\begin{aligned} \frac{\partial}{\partial t} (\bar{\rho} \tilde{u}_i) + \frac{\partial}{\partial x_j} (\bar{\rho} \tilde{u}_j \tilde{u}_i) = & - \frac{\partial \bar{p}}{\partial x_i} \\ & + \frac{\partial}{\partial x_j} \left[\bar{\tau}_{ij} - \overline{\rho u_j'' u_i''} \right] + \bar{\rho} g_i, \end{aligned} \quad (3)$$

where

$$\bar{\tau}_{ij} = \mu \left[\left(\frac{\partial \tilde{u}_i}{\partial x_j} + \frac{\partial \tilde{u}_j}{\partial x_i} \right) - \frac{2}{3} \frac{\partial \tilde{u}_l}{\partial x_l} \delta_{ij} \right], \quad (4)$$

$$\frac{\partial (\bar{\rho} \tilde{T})}{\partial t} + \frac{\partial (\tilde{u}_i \tilde{T})}{\partial x_i} = \frac{\partial}{\partial x_i} \left(\alpha \frac{\partial \tilde{T}}{\partial x_i} - \overline{\rho u_i'' T''} \right) \quad (5)$$

$$\bar{p} = \bar{\rho} R \tilde{T} \quad (6)$$

In this system of equations, ρ is the fluid density, t is time, x_i are the space cartesian coordinates in index notation, μ is the dynamic viscosity coefficient, α is the molecular thermal diffusivity, δ_{ij} is the Kronecker's delta operator, g_i is the acceleration due to gravity, T is the fluid temperature, u_i is the flow velocity, k is the thermal conductivity, p is the fluid pressure and τ is the fluid stress tensor. In these equations the tilde denotes the time-average of a quantity whereas quotation marks denote the fluctuation of a quantity in the sense of Favre (1965) decomposition. Similarly, overbar denotes the time-average of a quantity in the sense of Reynolds (1895) decomposition. Two new unknown quantities appear, respectively, in the momentum (3) and in the energy equations (5), defined by the correlations between velocity fluctuations, the so-called Reynolds Stress, given by the tensor $-\overline{\rho u_i'' u_j''}$, and by fluctuations of temperature and velocity, the so-called turbulent heat flux, defined by the vector $-\overline{\rho u_i'' T''}$.

The Reynolds stress of turbulent tensions is calculated by the $\kappa - \varepsilon$ model, proposed by Jones and Launder (1972) with the modifications introduced by Launder and Spalding (1974), given by

$$\begin{aligned} -\overline{\rho u_i'' u_j''} = \mu_t \left(\frac{\partial \tilde{u}_i}{\partial x_j} + \frac{\partial \tilde{u}_j}{\partial x_i} \right) \\ - \frac{2}{3} \left(\bar{\rho} \kappa + \mu_t \frac{\partial \tilde{u}_l}{\partial x_l} \right) \delta_{ij}, \end{aligned} \quad (7)$$

with

$$\kappa = \frac{1}{2} \overline{u_i'' u_i''}. \quad (8)$$

and

$$\mu_t = C_\mu \bar{\rho} \frac{\kappa^2}{\varepsilon} = \frac{1}{Re_t}. \quad (9)$$

The turbulent heat flux is modeled using the Fourier law and a turbulent Prandl number Pr_t equal to a constant value of 0.9 by the relation:

$$-\overline{\rho u_i'' T''} = \frac{\mu_t}{Pr_t} \frac{\partial \tilde{T}}{\partial x_i}. \quad (10)$$

In Eq. (9) C_μ is a constant of calibration of the model, equal to 0.09, κ represents the turbulent kinetic energy and ε is the rate of dissipation of the turbulent kinetic energy. Once κ and ε are additional variables, we need to know the transport equations. The transport equations of κ and ε were deduced by Jones and Launder (1972), and the closed system of equations of the $\kappa - \varepsilon$ model is given by:

$$\frac{\partial \bar{\rho}}{\partial t} + \frac{\partial (\bar{\rho} \tilde{u}_i)}{\partial x_i} = 0, \quad (11)$$

$$\begin{aligned} \frac{\partial (\bar{\rho} \tilde{u}_i)}{\partial t} + \tilde{u}_j \frac{\partial (\bar{\rho} \tilde{u}_i)}{\partial x_j} = & - \frac{\partial \bar{p}^*}{\partial x_i} \\ & + \frac{\partial}{\partial x_j} \left[\left(\frac{1}{Re} + \frac{1}{Re_t} \right) \left(\frac{\partial \tilde{u}_i}{\partial x_j} + \frac{\partial \tilde{u}_j}{\partial x_i} \right) \right] + \frac{1}{Fr} \bar{\rho} g_i, \end{aligned} \quad (12)$$

$$\begin{aligned} \frac{\partial (\bar{\rho} \tilde{T})}{\partial t} + \tilde{u}_j \frac{\partial (\bar{\rho} \tilde{T})}{\partial x_j} = \\ \frac{\partial}{\partial x_j} \left[\left(\frac{1}{Re Pr} + \frac{1}{Re_t Pr_t} \right) \frac{\partial \tilde{T}}{\partial x_j} \right], \end{aligned} \quad (13)$$

$$\begin{aligned} \frac{\partial (\bar{\rho} \kappa)}{\partial t} + \tilde{u}_i \frac{\partial (\bar{\rho} \kappa)}{\partial x_j} = \frac{\partial}{\partial x_i} \left(\frac{1}{Re} \frac{\partial \kappa}{\partial x_i} \right) \\ + \frac{\partial}{\partial x_i} \left(\frac{1}{Re_t \sigma_\kappa} \frac{\partial \kappa}{\partial x_i} \right) + \Pi - \bar{\rho} \varepsilon + \frac{\bar{\rho} \beta g_i}{Re_t Pr_t} \frac{\partial \tilde{T}}{\partial x_i}, \end{aligned} \quad (14)$$

$$\begin{aligned} \frac{\partial (\bar{\rho} \varepsilon)}{\partial t} + \tilde{u}_i \frac{\partial (\bar{\rho} \varepsilon)}{\partial x_j} = \frac{\partial}{\partial x_i} \left(\frac{1}{Re} \frac{\partial \varepsilon}{\partial x_i} \right) \\ + \frac{\partial}{\partial x_i} \left(\frac{1}{Re_t \sigma_\varepsilon} \frac{\partial \varepsilon}{\partial x_i} \right) + \frac{\varepsilon}{\kappa} (C_{\varepsilon 1} \Pi - C_{\varepsilon 2} \bar{\rho} \varepsilon) \\ + \frac{\varepsilon}{\kappa} \left(C_{\varepsilon 3} \frac{\bar{\rho} \beta g_i}{Re_t Pr_t} \frac{\partial \tilde{T}}{\partial x_i} \right), \end{aligned} \quad (15)$$

$$\bar{\rho} (1 + \tilde{T}) = 1, \quad (16)$$

where:

$$\frac{1}{Re_t} = C_\mu \bar{\rho} \frac{\kappa^2}{\varepsilon}, \quad (17)$$

$$\begin{aligned} \Pi = \frac{1}{Re_t} \left(\frac{\partial \tilde{u}_i}{\partial x_j} + \frac{\partial \tilde{u}_j}{\partial x_i} \right) \frac{\partial \tilde{u}_i}{\partial x_j} \\ - \frac{2}{3} \left(\bar{\rho} \kappa + \frac{1}{Re_t} \frac{\partial \tilde{u}_l}{\partial x_l} \right) \delta_{ij} \frac{\partial \tilde{u}_i}{\partial x_j}, \end{aligned} \quad (18)$$

$$p^* = \bar{p} + \frac{2}{3} \left[\left(\frac{1}{Re} + \frac{1}{Re_t} \right) \frac{\partial \tilde{u}_i}{\partial x_i} + \bar{\rho} \kappa \right] \quad (19)$$

with the model constants given by:

$$C_\mu = 0,09, C_{\varepsilon 1} = 1,44, C_{\varepsilon 2} = 1,92,$$

$$C_{\varepsilon 3} = 0,288, \sigma_\kappa = 1, \sigma_\varepsilon = 1,3, Pr_t = 0,9.$$

Wall Functions

The $\kappa - \varepsilon$ turbulence model is incapable of properly representing the laminar sub-layer and the transition regions of the turbulent boundary layer. To solve this inconvenience, the solution adopted in this work is the use of wall laws, capable of properly representing the flow in the inner region of the turbulent boundary layer.

There are four velocity and two temperature wall laws implemented on the code Turbo 2D. The laws used in this simulation are explained below, except for the classical log law whose further explanations are unnecessary.

Velocity wall law of Mellor (1966)

Deduced from the mean equation of Prandtl for the turbulent boundary layer and considering the pressure gradient term for integration, this wall function is a primary approach to flows that suffer influence of adverse pressure gradients. Its equations are, respectively, for the laminar and turbulent regions

$$u^* = y^* + \frac{1}{2} p^* y^{*2}, \quad (20)$$

$$u^* = \frac{2}{K} \left(\sqrt{1 + p^* y^*} - 1 \right) + \frac{1}{K} \left(\frac{4y^*}{2 + p^* y^* + 2\sqrt{1 + p^* y^*}} \right) + \xi_{p^*}, \quad (21)$$

where the asterisk upper-index indicates dimensionless quantities of velocity u^* , pressure gradient p^* and distance to the wall y^* as functions of scaling parameters at the near wall region, K is the Von Karman constant and ξ_{p^*} is Mellor's integration constant which is a function of the near-wall dimensionless pressure gradient.

For calculation purposes the intersection of both regions is considered to be the same as the log law expressions, where $y^* = 11,64$. The relations between the dimensionless near wall properties and the friction velocity u_f are:

$$y^* = \frac{y u_f}{\nu}, u^* = \frac{\tilde{u}_x}{u_f} \text{ and } p^* = \frac{1}{\bar{\rho}} \frac{\partial \bar{p}}{\partial x} \frac{\nu}{u_f^3}. \quad (22)$$

The friction velocity is calculated by the relation:

$$u_f = \left(\frac{1}{Re} + \frac{1}{Re_T} \right) \frac{\partial u_i}{\partial x_j} - \frac{1}{\rho} \frac{\partial P}{\partial x_i} \delta_{ij} \quad (23)$$

In Eq. (21) the term ξ_{p^*} is a value obtained from the integration process proposed by Mellor (1966) and is a function of the dimensionless pressure gradient. Its values are obtained through interpolation of those obtained experimentally by Mellor, shown in Table 1.

Table 1. Mellor's integration constant (1966).

p^*	-0.01	0.00	0.02	0.05	0.10	0.20
ξ_{p^*}	4.92	4.90	4.94	5.06	5.26	5.63
p^*	0.25	0.33	0.50	1.00	2.00	10.00
ξ_{p^*}	5.78	6.03	6.44	7.34	8.49	12.13

Velocity wall law of Nakayama and Koyama (1984)

In their work Nakayama and Koyama (1984) proposed a derivation of the mean turbulent kinetic energy equation, that resulted in an expression to evaluate the velocity near solid boundaries. Using experimental results and those obtained by Stratford (1959), the derived equation is

$$u^* = \frac{1}{K^*} \left[3(t - t_s) + \ln \left(\frac{t_s + 1}{t_s - 1} \frac{t - 1}{t + 1} \right) \right], \quad (24)$$

with

$$t = \sqrt{\frac{1 + 2\tau^*}{3}}, \quad \tau^* = 1 + p^* y^*,$$

$$K^* = \frac{0,419 + 0,539 p^*}{1 + p^*} \quad \text{and} \quad y_s^* = \frac{e^{K^* C}}{1 + p^* 0,34}, \quad (25)$$

where K^* is the expression for the Von Karman constant modified by the presence of adverse pressure gradients, τ^* is a dimensionless shear stress, $C = 5,445$ is the log-law constant and the parameter t_s is a value of t at a position y_s^* .

Velocity wall law of Cruz and Silva Freire (1998)

Analyzing the asymptotic behavior of the boundary layer flow under adverse pressure gradients, Cruz and Silva Freire (1998) derived an expression for the velocity in the inner region of turbulent boundary layer. The solution of the asymptotic approach is

$$u = \frac{\tau_w}{|\tau_w|} \frac{2}{K} \sqrt{\frac{\tau_w}{\rho} + \frac{1}{\rho} \frac{dp_w}{dx}} y + \frac{\tau_w}{|\tau_w|} \frac{u_f}{K} \ln \left(\frac{y}{L_c} \right)$$

$$\text{with } L_c = \frac{\sqrt{\left(\frac{\tau_w}{\rho} \right)^2 + 2 \frac{\nu}{\rho} \frac{dp_w}{dx} u_f - \frac{\tau_w}{\rho}}}{\frac{1}{\rho} \frac{dp_w}{dx}} \quad (26)$$

where the sub-index w indicates the properties at the wall, K is the Von Karman constant, L_c is a length scale parameter and u_f is the friction velocity.

The proposed equation for the velocity, equation (26), has a behavior similar to the log law far from the separation and reattachment points, but, close to the separation point, it gradually tends to Stratford's equation (1959).

Temperature wall law of Cheng and Ng (1982)

In this work it is used the temperature wall law of Cheng and Ng (1982). For the calculation of the temperature profile in the near wall region, Cheng and Ng (1982) derived an expression similar to the logarithmic law for velocity. For the laminar and turbulent regions, the equations are respectively

$$\begin{aligned} \frac{(T_0 - T)_y}{T_f} &= y^* Pr \quad \text{and} \\ \frac{(T_0 - T)_y}{T_f} &= \frac{1}{K_{Ng}} \ln(y^*) + C_{Ng} \\ \text{with } y^* &= \frac{u_f y}{\nu} \end{aligned} \tag{27}$$

where T_0 is the environmental temperature, y is the normal distance up to the wall, ν is the cinematic viscosity and T_f is the friction temperature, as defined by Brun (1988)

$$T_f = \frac{1}{u_f} \left[\left(\frac{1}{RePr} + \frac{1}{Re_T Pr_T} \right) \frac{\partial \tilde{T}}{\partial x_j} \right]_{\delta} \tag{28}$$

and the friction velocity u_f is calculated by Eq. (23). The intersection of these regions are at $y^* = 15, 96$ and the constants K_{Ng} and C_{Ng} are, respectively, 0, 8 and 12, 5.

The Heat Flux Boundary Condition And The $\kappa - \varepsilon$ Model

As discussed before, imposing a heat flux boundary condition on the wall in a high Reynolds turbulence model, such as the classical $\kappa - \varepsilon$, requires a special treatment since there are no heat flux wall functions available. This work proposes a new method to solve this inconvenience without the need of creating a heat flux wall law. The main idea is to use the Colburn (1933) analogy, Eq. (29), to estimate the Stanton number for non-detached boundary layers.

$$St_x = \frac{C_{fx}}{2Pr^{\frac{2}{3}}}, \tag{29}$$

where C_{fx} is the local friction coefficient and the local Stanton number can be evaluated by

$$St_x = \frac{q_x}{\rho c_p u_{\infty} (T_w - T_{\infty})}, \tag{30}$$

where, for a flat plate

$$q_x = -k \left(\frac{\partial T}{\partial y} \right)_{y=0}. \tag{31}$$

By Eq. (30) it is possible to convert an imposed heat flux on the wall into an equivalent wall temperature by knowing the behavior of the local Stanton number, since

$$T_w = T_{\infty} + \frac{q_x}{\rho C_p u_{\infty} St_x}. \tag{32}$$

If there is an unheated starting length, so the thermal boundary layer begins its development under a pre-existing velocity boundary layer an adjustment is necessary to take into account this peculiarity of the flow. The adjust proposed by Kays and Crawford (1993) can be done on Eq. (29) resulting in the Eq. (36),

$$St_x = \frac{C_{fx}}{2Pr^{\frac{2}{3}}} \left(\frac{\delta_u}{\delta_T} \right)^{\frac{1}{7}}, \tag{33}$$

where δ_u and δ_T denotes, respectively, the velocity and thermal boundary layer thickness.

In equation (30) an accurate calculation of the temperature gradient is a difficult task since the use of wall laws produces the loss of some information in the wall region. On the other hand, this difficulty can be avoided by employing equations (29) or (36), where the local friction coefficient C_{fx} is calculated with the use of the friction velocity u_f , which is calculated by equation (23), so:

$$\begin{aligned} \frac{C_{fx}}{2} &= \frac{\tau_w}{\rho u_{\infty}^2} \quad \text{with} \quad \tau_w = \rho u_f^2 \\ \text{and} \quad C_{fx} &= 2 \frac{u_f^2}{u_{\infty}^2}. \end{aligned} \tag{34}$$

By these calculations it is possible to estimate, with a good accuracy, the heat transfer rates in turbulent flows where the boundary layer is well structured, for example, in flows over flat plates and other geometries that don't generate boundary layer detachment.

The problem in using this formulation happens when we analyze the flow inside or at downstream of a recirculation region, where the boundary layer is not well structured and the use of analogies is not a viable alternative. In these cases, Gontijo and Fontoura Rodrigues (2009) developed an expression using a previously experimental work of Vogel and Eaton (1985), where the authors studied a turbulent flow over a heated backward facing step that had a condition of a constant heat flux imposed on its lower wall. The relation obtained is expressed by Eq. (35).

$$St(x^*) = 0,00106 + 0,00912x^* - 0,00895x^{*2} + 0,00233x^{*3},$$

with

$$x^* = \frac{x - x_d}{x_r - x_d}, \tag{35}$$

where x defines the local coordinate in the flow direction, x_d is the detachment point and x_r is the reattachment point.

Expression (35) presents good results in other geometries, different from the backward facing step, as the next section will show.

Results

Several test cases were used to validate this methodology in order to show its generality. First it is shown the good performance of analogies in cases where there is no boundary layer detachment. Following are addressed problems of using classical analogies when the boundary layer is not well structured. Thereafter, it is shown the arguments taken into account to develop a new approach to calculate the Stanton number inside a recirculation region and, finally, this approach is tested for different geometries that induce boundary layer detachment. A mesh study was done for each test case and more details on the numerical process can be found in the Master's Dissertation of Gontijo (2009).

Use of analogies on flat plates with unheated starting lengths and low temperature gradients

First it is shown the performance of the Colburn analogy in the estimation of the local Stanton number for four different test cases, based on the experimental works of Taylor et al. (1990). In this work the authors made several measurements of the local Stanton number over a heated flat plate. The plate had $2.4m$ long. The flow is considered two-dimensional in the middle section and the velocity of the free stream flow is $U_\infty = 28m/s$. The results presented in Fig. (1) show the behavior of four different test cases, varying the initial unheated starting length.

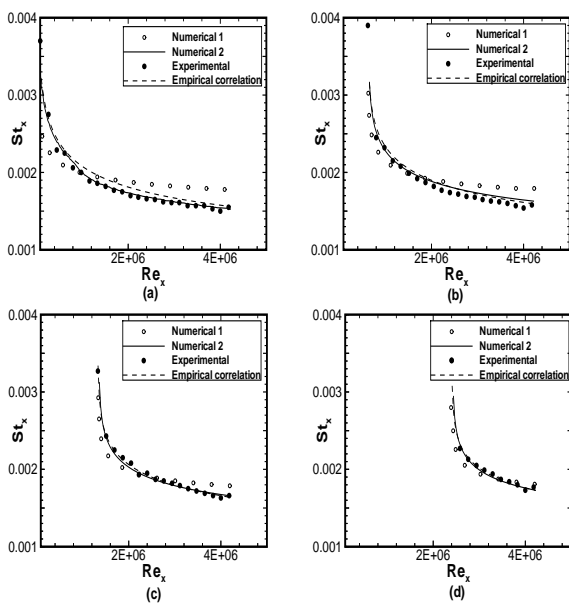


Figure 1. Local Stanton number for Taylor et al. (1990) test case. $U_\infty = 28$ - Isothermal plate (a), $\xi=0,36$ m (b), $\xi=0,76$ m (c) and $\xi=1,36$ m (d).

In the legend the experimental result is obtained from the work of Taylor et al. (1990), empirical correlation denotes the Kays and

Crowford (1993) correlation, given by

$$St_x = \frac{Cf_x}{2Pr^{2/3}} \left[1 - \left(\frac{\xi}{x} \right)^{9/10} \right]^{-1/9}, \quad (36)$$

where x is the distance from the beginning of the plate and ξ is the unheated starting length. The numerical value of the local Stanton number was calculated by two different ways, using Eqs. (30) and (36) called in Fig. (1), respectively, numerical 1 and numerical 2. The main idea of the works of Taylor et al. (1990) is to evaluate the influence of a thermal boundary layer starting over a developed velocity boundary layer in the behavior of the heat transfer rates over a plate with low temperature gradients. In these cases, there is a difference of $18K$ between the temperature of the plate and of the free stream flow. The numerical P1-isoP2 mesh used to execute the simulations had 18447 nodes and 35872 elements. In this case the wall law used for velocity was the classic logarithm law and for temperature the wall law of Cheng and Ng (1982), since there are no significative pressure gradients imposed by this geometry. It is possible to notice that the use of the Colburn (1933) analogy calculated by Eq. (36) produces better results. The explanation for this behavior consists on the fact that the derivatives of temperature in the normal direction of the plate are not taken on the wall, since the use of a high Reynolds model restrict the numerical simulation to a certain distance above it.

Analogies in an isothermal flat plate with high temperature gradients

In order to validate the use of the Colburn (1933) analogy in problems where the temperature and velocity fields are coupled due to a high temperature gradient, a simulation of a problem first studied by Ng (1981) is presented. In this test case a flat plate of $0.25m$ long, heated in a constant temperature of $1250K$, receives a flow of air with a free stream velocity of $10,7m/s$ and with an uniform temperature of $293K$. In this work the range of the local Reynolds number is placed between $5.0 \cdot 10^5 < Re_x < 7.8 \cdot 10^5$. There is a difference of $957K$ between the temperature of the plate and of the free stream flow. It was used a P1-isoP2 mesh with 6499 nodes and 12672 elements. The simulation was done with the classic wall law for velocity and the wall law of Cheng and Ng (1982) for temperature. Figure (2) shows the variation of the local Stanton number through the plate calculated by the same way as those from the Taylor et al. (1990) test case.

In the legend of Fig. (2) the experimental values are taken from the work of Ng (1981) and the numerical values are obtained by the same way that in the Taylor et al. (1990) test case. The behavior observed is the same, the use of the Colburn (1933) analogy calculated by Eq. (36) is the best option to estimate the heat transfer rates. It is important to notice that the Colburn analogy works well even when the temperature gradients involved are very strong.

The use of analogies in a recirculation region

To check the behavior of the heat transfer rates inside a recirculation region and the performance of analogies in this situation, it

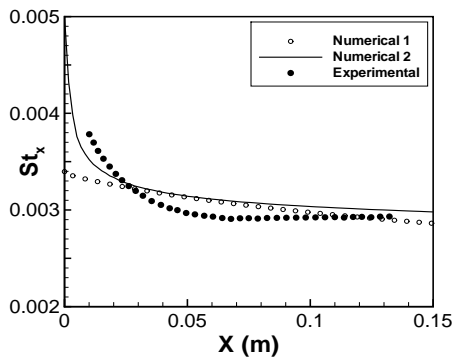


Figure 2. Local Stanton number for Ng (1981) test case.

was selected a test case based on the works of Liou et al. (1992). In this test case, artificial roughness elements called *ribs* are used to induce the flow separation, increasing the turbulence levels and, by consequence, the heat transfer rates. The ribbed channel studied in this work presents a Reynolds number of 12600. The velocity on which the Reynolds number was calculated is $7.4m/s$ and the height of the rib is $0.008m$. The P1-isoP2 mesh used on the simulations had 3739 nodes and 7200 elements. In the experimental work of Liou et al. (1992), the rib was made of aluminum and it was heated by a thermal film in its underside, providing a condition of constant heat flux. The top part of the channel was insulated, so an adiabatic wall was created. The height of the rib represents twenty percent of the height of the channel. Figure (3) shows the behavior of the heat transfer rates along the channel. In the legend of Fig. (3) the experimental values are taken from the work of Liou et al. (1992).

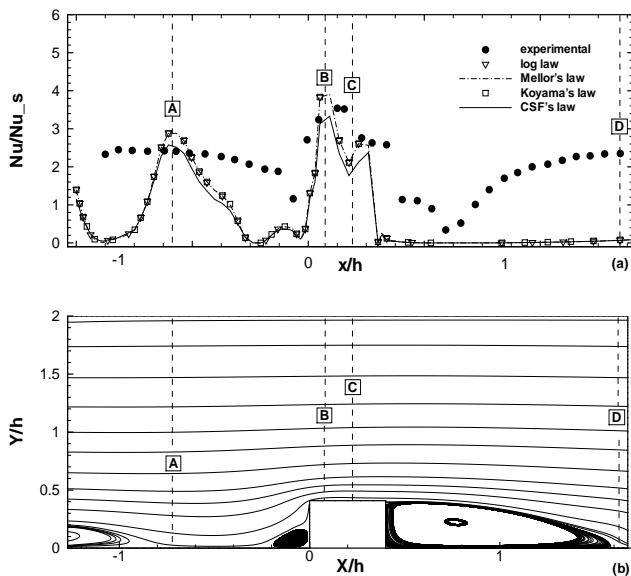


Figure 3. Nusselt number along the bottom wall (a), structure of the recirculation regions (b).

In this work, the wall heat flux is calculated in the non dimen-

sional form of the Nusselt number that for a channel can be calculated by the following relation:

$$Nu_x = \frac{2q_x Pr H}{\mu C_p (T_w - T_{bulk})} \tag{37}$$

In the equation above, Nu_x represents the local Nusselt number, q_x is the local heat flux, Pr is the Prandtl number of the fluid, H is the height of the channel, and T_w is the temperature of the wall. Combining Eq. (37) with the Colburn (1933) analogy, Eq. (30), and with the definition of the local Stanton number, where the bulk temperature may be taken as

$$T_{bulk} = \frac{T_w + T_\infty}{2}, \tag{38}$$

it is possible to establish a relation between the local Nusselt number and the friction velocity as

$$Nu_x = \frac{4Pr^{1/3} u_{fx}^2 H}{\nu u_\infty}. \tag{39}$$

The values of Nu_s , shown in Fig. (3), are the local Nusselt numbers for a channel without the presence of the Ribs, calculated by the Dittus-Boelter equation. It is possible to observe a good agreement between numerical and experimental data in non detached regions (places A, B and C). Inside the recirculation zones, the use of the Colburn analogy does not present good results. This was already expected, since analogies between fluid friction and heat transfer can only be done in a well structured boundary layer. The results of Fig. (3) show the necessity of an alternative treatment to estimate, with a good accuracy, the behavior of the local Stanton number in regions of the flow where the boundary layer is not well structured, like inside recirculation zones and after the reattachment of the boundary layer, as the following test case will illustrate.

An approach to estimate the Stanton number in detached flows

In order to propose a new methodology to estimate the local Stanton number inside a recirculation region, the experimental work of Vogel and Eaton (1985) was set as the benchmark to develop this approach. In this test case a backward facing step, with a height of $0.038m$ is heated in the bottom plate with a constant heat flux of $270W/m^2$. The Reynolds number based on the height of the step is 27023. The free stream velocity of the flow is $11.3m/s$. The P1-isoP2 mesh used to execute the simulation has 4191 nodes and 8016 elements. Figure (4) shows the behavior of the local Stanton number when calculated by the use of the Colburn analogy. This behavior suggests that after the reattachment point the boundary layer is being restructured. This restructure occurs in a region that has approximately the same length of the recirculation region.

Results in Figs. (4.a) and (5) marked as experimental are taken from the work of Vogel and Eaton (1985). The results of Fig. (4.a) suggest that it is possible to calibrate a polynomial relation to calculate the local Stanton number, inside the recirculation region from

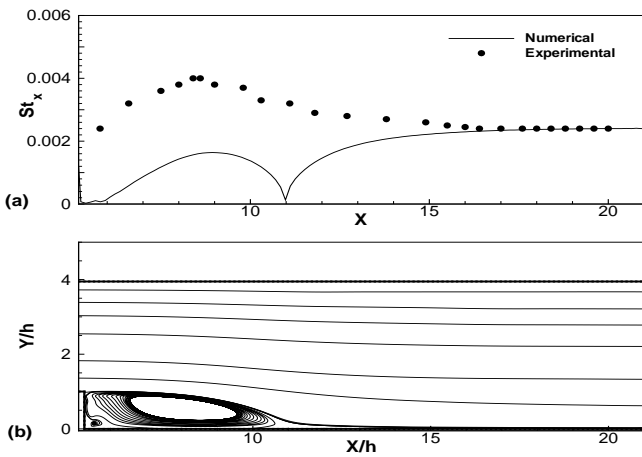


Figure 4. Numerical and experimental behavior of the Stanton number (a), streamlines of the flow (b).

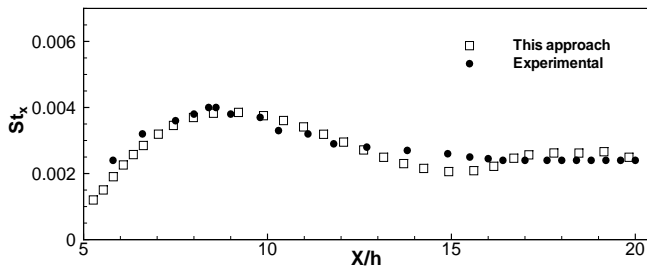


Figure 5. Adjusts obtained by the proposed relation.

the detachment point to a distance of twice the recirculation zone length, based on the physical reality of the backward facing step of Vogel and Eaton. This relation is given by Eq. (35). By using this equation the behavior of the local Stanton number, in a simulation done with the Cruz and Silva Freire wall law, is shown in Fig. (5). The adjust obtained with Eq. (35) shows a good accuracy between numerical and experimental values and the transition from the use of this equation to the calculation with the Colburn analogy is smooth, after the restructuring region of the boundary layer. It is important to say that the necessary length for the boundary layer restructuring is still an open problem and needs further studies. However, this methodology turns viable the simulation of turbulent thermal flows with the high Reynolds $\kappa - \epsilon$ model with wall laws and heat flux boundary conditions. In order to validate this methodology to other geometries with boundary layer detachment, the next section shows its performance in an asymmetric plane diffuser and on a smooth hill.

Extension of this new approach to other detached flows induced by different geometries

In order to extend this methodology to other geometries, two new test cases were proposed, based on studies of the asymmetric plane

diffuser of Buice and Eaton (1995) and the turbulent flow over a 2D hill, studied by Loureiro et al. (2007). The boundary conditions used to execute these simulations are illustrated in Figs. (6) and (7).

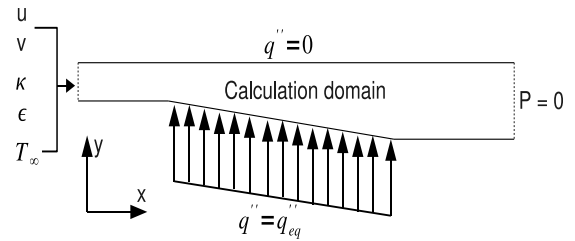


Figure 6. Geometry and boundary conditions of the Buice and Eaton (1995) diffuser.

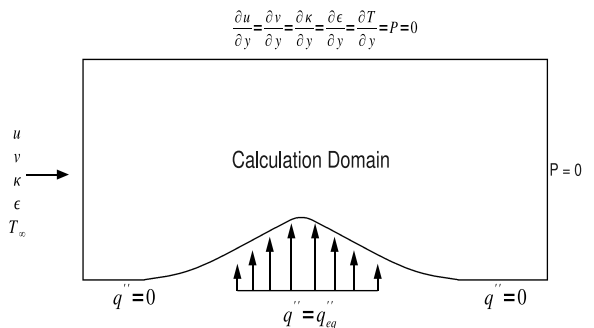


Figure 7. Geometry and boundary conditions of the Loureiro et al. (2007) 2D hill.

In the experimental works of Buice and Eaton (1995) and Loureiro et al. (2007), the thermal field is not considered. They studied only the dynamical field. What was done to create two new test cases based on these experimental works was to calculate first the dynamical field of these flows, without inputting any thermal boundary condition. Then, a simulation with an imposed constant temperature on the wall was executed. After this step, the equivalent thermal energy injected in the flow is calculated by measuring the temperature profiles before and after the heated wall. After this step, an equivalent heat flux was calculated and imposed in the same wall, where the constant temperature condition was imposed. By doing this procedure it is expected that the same energy injected in the flow, by the constant temperature boundary condition, should be injected by the equivalent constant heat flux condition. It is important to say that in both cases occur the boundary layer detachment. In order to obtain an accurate behavior of the velocity and temperature fields inside the recirculation regions, the law of the wall of Cruz and Silva Freire (1998) was used in both cases. This law was the one with the best performance among all the laws of the wall tested. These results were published in the master's dissertation of Gontijo (2009), where more details can be found.

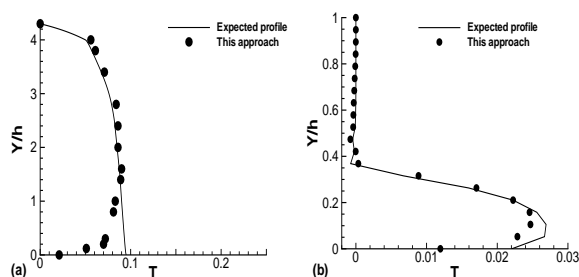


Figure 8. Temperature profiles in the asymmetric diffuser of Buice and Eaton (1995) - $X/h=26$ (a) and in the 2D hill of Loureiro et al. (2007) in $X/h=6.5$ (b).

Figure (8) illustrates, respectively, the temperature profiles taken after the heated walls for the asymmetric plane diffuser of Buice and Eaton (1995) and the 2D hill of Loureiro et al. (2007) test cases. The expected profile line indicates a temperature profile taken when an equivalent constant temperature is imposed, more details are given in the master's dissertation of Gontijo (2009). This approach is able to predict the equivalent wall temperature inside the recirculation regions of flows over distinct boundary geometries, even when the mechanism responsible by the boundary layer detachment is a very smooth adverse pressure gradient. More details over the process of development of this new methodology are given by Gontijo and Fontoura Rodrigues (2009). It is important to notice that the temperature profiles should not be exactly the same when simulations are taken using a constant temperature and a constant heat flux boundary condition, even if the energy injected by both boundary conditions is the same. The energy injected in the flow, associated with the integral of the temperature profile should be the same instead. The error on the energy injected by both boundary conditions, obtained with this methodology based on the physical reality of the backward facing step and extended to other geometries is 0.21% for the diffuser and 0.06% for the smooth hill.

Conclusions

This work proposed, implemented and validated, successfully, a original numerical methodology used to impose heat flux boundary conditions in the high Reynolds $\kappa - \varepsilon$ model, without the need to create a heat flux law of the wall. Past works done by the authors were used to develop this methodology based on the employment of classical analogies between fluid friction and heat transfer on the wall. The test case used to develop this methodology and also to understand the main obstacles of this approach was the Vogel and Eaton (1985) backward facing step. The advances done based in this test case were then tested in two other geometries and showed that this methodology can be extended to distinct geometries, even when the detached is induced by smooth adverse pressure gradients. One of the aspects that can be better studied is the necessary length to the restructuring of the boundary layer after the detachment, even though in the studied test cases the adopted standard considered in

this work has provided good results.

Acknowledgements

The authors are grateful by the support given by the Conselho Nacional de Desenvolvimento Científico e Tecnológico, CNPq and by the professors, students and members of the research group Vortex - Group of Fluid Mechanics of Complex Flows of the University of Brasília.

References

- Boussinesq, J., 1877, "Théorie de l'écoulement Tourbillant", Mem. Présentés par Divers Savants Acad. Sci. Inst. Fr., Vol. 23, pp. 46-50.
- Buffat, M., 1981, "Formulation moindre carrés adaptées au traitement des effets convectifs dans les équation de Navier-Stokes", Doctorat thesis, Université Claude Bernard, Lyon, France.
- Buice, C. and Eaton, J., 1995, "Experimental investigation of flow through an asymmetric plane diffuser", Annual Research Briefs - 1995, Center of Turbulence Research, Stanford University/ NASA Ames, pp. 117-120.
- Brison, J.F., Buffat, M., Jeandel, D., Serrer, E., 1985, "Finite elements simulation of turbulent flows, using a two equation model", Numerical methods in laminar and turbulent flows, Swansea. Pineridge Press.
- Brun, G., 1988, "Développement et application d'une méthode d'éléments finis pour le calcul des écoulements turbulents fortement chauffés", Doctorat thesis, Laboratoire de Mécanique des Fluides, Ecole Centrale de Lyon, France.
- Chen, C.J. and Jaw, S.Y., 1998, "Fundamentals of Turbulence Modeling", Taylor and Francis, New York.
- Cheng, R.K. and Ng, T.T., 1982, "Some aspects of strongly heated turbulent boundary layer flow", *Physics of Fluids*, Vol. 25(8).
- Colburn, A.P., 1933, "A method for correlating forced convection heat transfer data and a comparison with fluid friction", *Transaction of American Institute of Chemical Engineers*, Vol. 29, pp. 174-210.
- Cruz, D.O.A., Silva Freire, A.P., 1998, "On single limits and the asymptotic behavior of separating turbulent boundary layers", *International Journal of Heat and Mass Transfer*, Vol. 41, N° 14, pp. 2097-2111.
- Favre, A., 1965, "Equations de gaz turbulents compressibles", *Journal de mécanique*, Vol. 3 and Vol. 4.
- Fontoura Rodrigues, J.L.A., 1990, "Méthode de minimisation adaptée à la technique des éléments finis pour la simulation des écoulements turbulents avec conditions aux limites non linéaires de proche paroi", Doctorat thesis, Ecole Centrale de Lyon, France.
- Gontijo, R.G. and Fontoura Rodrigues, J.L.A., 2006, "Numerical modeling of the heat transfer in the turbulent boundary layer", Encit, 2006.
- Gontijo, R.G. and Fontoura Rodrigues, J.L.A., 2007, "Numerical modeling of a turbulent flow over a 2D channel with a rib-roughened wall", Cobem, 2007.
- Gontijo, R.G. and Fontoura Rodrigues, J.L.A., 2008, "Implementation and validation of a methodology used to impose heat flux

boundary conditions in a high Reynolds turbulence model”, Encit, 2008.

Gontijo, R.G. and Fontoura Rodrigues, J.L.A., 2009, “Thermal boundary conditions based on the use of analogies. A numerical study”, Cobem, 2009.

Huges, T.J.R. and Brooks, A., 1979, “A multi-dimensional upwind scheme with no crosswind diffusion”, in “Finite Element Methods for Convection Dominated Flows”, ASME - AMD 34, New York.

Jones, W. and Launder, B.E., 1972, “The prediction of laminarization with a two equations model of turbulence”, *International Journal of Heat and Mass Transfer*, Vol. 15, pp. 301-314.

Kays, W.M., Crawford, M.E., 1993, “Convective Heat and Mass Transfer”, McGraw Hill, INC., USA.

Kelly, D.W., Nakazawa, S., Zienkiewicz, O.C., Heinrich, J., 1976, “A note on upwind and anisotropic balancing dissipation in finite element approximations to convective diffusion problems”, *International Journal for Numerical Method in Engineering*, **15**, Vol. 11, pp.1705-1711.

Launder, B.E. and Spalding, D.B., 1974, “The numerical computation of turbulent flows”, *Computational Methods in Applied Mechanical Engineering*, Vol. 3, pp. 269-289.

Loureiro, J.B.R, Soares, D.V, Fontoura Rodrigues, J.L.A, Silva Freire, A.P, Pinho, F.T, 2007, “Water tank and numerical model studies of flow over 2-D hill”, *Boundary Layer Meteorology*, Vol. 122, Serie 2 , pp.343-365.

Mellor, G.L., 1966, “The effects of pressure gradients on turbulent flow near a smooth wall”, *Journal of Fluid Mechanics*, Vol. 24, N^o 2, pp. 255-274.

Nakayama, A., Koyama, H., 1984, “A wall law for turbulent boundary layers in adverse pressure gradients”, *AIAA Journal*, Vol. 22, N^o 10, pp. 1386-1389.

Reynolds, O., 1895, “On The Dynamical Theory of Incompressible Viscous Fluids and the Determination of the Criterion”, *Philosophical Transactions of the Royal Society of London, Series A*, Vol. 186, p. 123.

Taylor, R.P. , Love, P.H. , Coleman, H.W. and Hosni, M.H., 1990, “Heat Transfer Measurements in Incompressible Turbulent Flat Plate Boundary Layers With Step Wall Temperature Boundary Conditions”, *Journal of Heat Transfer*, Vol. 112, pp 245-247.

Vogel, J.C., Eaton, J.K., 1985, “Combined heat transfer and fluid dynamic measurements downstream of a backward-facing step”, *Journal of heat transfer*, November, Vol. 107, pp 922-929.